International Journal for Innovative Engineering and Management Research
A Peer Revieved Open Access International Journal
www.ijiemr.org

COPY RIGHT

IJIEMR Transactions, online available on 16th June 2017. Link :
http://www.ijiemr.org/downloads.php?vol=Volume-6&issue=ISSUE-4

Title: Design And Analysis Of Three-Phase Transformer Less Grid-Connected PV Inverters.

Volume 06, Issue 04,Page No: 1029 – 1039.

Paper Authors

*** V.SIVA LINGAM, **D.PRAKASA RAO.**

* Chaitanya Institute Of Science And Technology.

USE THIS BARCODE TO ACCESS YOUR ONLINE PAPER

To Secure Your Paper As Per UGC Guidelines We Are Providing A Electronic Bar Code

International Journal for Innovative Engineering and Management Research
A Peer Revieved Open Access International Journal
www.ijiemr.org

DESIGN AND ANALYSIS OF THREE-PHASE TRANSFORMER LESS GRID-CONNECTED PV INVERTERS

***V.SIVA LINGAM, **D.PRAKASA RAO**

PG Scholar, Dept Of EEE, Chaitanya Institute Of Science And Technology,

KAKINADA,East Godavari (Dt); A.P, India.

Assistant Professor, Dept Of EEE, Chaitanya Institute Of Science And Technology,

KAKINADA,East Godavari (Dt); A.P, India.

ABSTRACT:

Three-phase transformer less inverter is widely used in low power photovoltaic (PV) grid-connected systems due to its small size, high efficiency and low cost. When no transformer is used in a grid connected photovoltaic (PV) system, a galvanic connection between the grid and PV array exists. In these conditions, dangerous leakage currents (common-mode currents) can appear through the stray capacitance between the PV array and the ground. The former, in order to create a galvanic isolation between the input and the output include a transformer (mandatory in some countries) that limits the whole system performances in terms of efficiency, weight, size and cost. On the contrary, transformer less inverters do not present any isolation and are characterized by little size, lower cost and higher efficiency (more than 2% higher). Nevertheless, the lack of transformers leads to leakage currents that can be harmful to the human body, as well as for the whole conversion system integrity. In order to avoid the leakage currents, various Transformer less inverters have been proposed using different topologies to generate constant common mode voltage. In this paper, various recently-proposed transformer less PV inverters are investigated. Their performances are compared and analyzed.

Index Terms: Common-mode voltage (CMV), leakage current, photovoltaic (PV) system, transformer less.

I. INTRODUCTION

Today, the energy demand is increasing due to the rapid increase of the human population and fast-growing industries. Hence, renewable energy plays an important role to replace traditional natural resources such as fuel and coal. Photovoltaic (PV) energy has recently become a common interest of research because it is free, green, and inexhaustible [1]–[2]. Furthermore, PV systems are now more affordable due to government incentives, advancement of power electronics and semiconductor technology and cost reduction in PV modules [3], [4].

Generally, there are two types of grid-connected PV systems, i. e., those with transformer and without transformer. The transformer used can be high frequency (HF) transformer on the dc side or low frequency transformer on the ac side [5]. Besides stepping up the voltage, it plays an important role in safety purpose by providing galvanic isolation, and thus eliminating leakage current and avoiding dc current injection into the grid. Nevertheless, the transformers are bulky,

International Journal for Innovative Engineering and Management Research
A Peer Revieved Open Access International Journal
www.ijiemr.org

heavy, and expensive. Even though significant size and weight reduction can be achieved with HF transformer, the use of transformer still reduces the efficiency of the entire PV system [6]. Hence, transformer less PV systems is introduced to overcome these issues. They are smaller, lighter, lower in cost, and highly efficient [7]. High frequency common-mode (CM) voltages must be avoided for a transformer less PV grid-connected inverter because it will lead to a large charge/discharge current partially flowing through the inverter to the ground. This CM ground current will cause an increase in the current harmonics, higher losses, safety problems, and electromagnetic interference (EMI) issues For a grid connected PV system, energy yield and payback time are greatly dependent on the inverter's reliability and efficiency, which are regarded as two of the most significant characteristics for PV inverters. In order to minimize the ground leakage current and improve the efficiency of the converter system, transformer less PV inverters utilizing unipolar PWM control have been presented [8]–[10]. The weighted California Energy Commission (CEC) or European Union (EU) efficiencies of most commercially available and literature-reported single-phase PV transformer less inverters are in the range of 96–98% The reported system peak and CEC efficiencies with an 8-kW converter system from the product datasheet is 98. 3% and 98%, respectively, with 345-V dc input voltage and a 16-kHz switching frequency.

However, this topology has high conduction losses due to the fact that the current must conduct through three switches in series during the active phase. Another disadvantage of the H5 is that the line-frequency switches S1 and S2 cannot utilize MOSFET devices because of the MOSFET body diode's slow reverse recovery. Replacing the switch S5 of the H5 inverter with two split switches S5 and S6 into two phase legs and adding two freewheeling diodes D5 and D6 for freewheeling current flows, the H6 topology was proposed in [12]. The H6 inverter can be implemented using MOSFETs for the line frequency switching devices, eliminating the use of less efficient IGBTs. The reported peak efficiency and EU efficiency of a 300 W prototype circuit were 98. 3% and 98.1%, respectively, with 180 V dc input voltage and 30 kHz switching frequency [13].

In order to address these two key issues, a new inverter topology is proposed for three-phase transformer less PV grid-connected systems in this paper. The proposed transformer less PV inverter features: 1) high reliability because there are no shoot-through issues, 2) low output ac current distortion as a result of no dead-time requirements at every PWM switching commutation instant as well as at grid zero-crossing instants, 3) minimized CM leakage current because there are two additional ac-side switches that decouple the PV array from the grid during the freewheeling phases, and 4) all the active switches of the proposed converter can reliably employ super junction MOSFETs since it never has the chance to induce MOSFET body diode reverse recovery. As a result of the low conduction and switching losses of the super junction MOSFETs, the proposed converter can be designed to operate at higher switching frequencies while maintaining high system efficiency. Higher switching frequencies reduce the ac-current ripple and the size of passive components [14].

II. COMMON-MODE BEHAVIOR AND LEAKAGE CURRENT REDUCTION METHODS

When the transformer is removed from the inverter, a resonant circuit is formed as shown in Fig.1 (a). This resonant circuit includes stray capacitance (CPV), the filter inductors (L1 and L2), and leakage current (IL). Here, the power converter is represented by a block with four

International Journal for Innovative Engineering and Management Research
A Peer Revieved Open Access International Journal
www.ijiemr.org

terminals to allow a general representation of various converter topologies. On the dc side, P and N are connected to the positive and negative rail of the dc-link, respectively; while on the ac side, terminals A and B are connected to the single-phase grid via filter inductors. From the view point of the grid, the power converter block shown in Fig.1.(a) can be considered as voltage sources, generating voltage VAN and VBN.

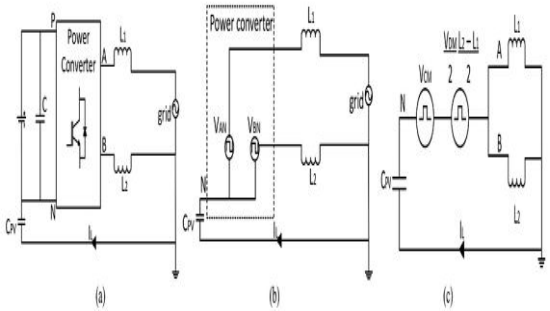

Fig.1. Common-mode model for single-phase grid-connected inverter. (a) Full model. (b) Simplified model. (c) Simplified common-mode model.

Hence, regardless of the conversion structure, this power converter block can be simplified into the equivalent circuit which consists of VAN and VBN as shown in Fig.2. (b). The leakage current is thus a function of VAN, VBN, grid voltage, filter inductance, and stray capacitance. The CMVVCM and differential-mode voltage VDM can be defined as

$$V_{CM} = \frac{V_{AN} + V_{BN}}{2} \quad (1)$$

$$V_{DM} = V_{AN} - V_{BN} \quad (2)$$

Rearranging (1) and (2), the output voltages can be expressed in terms of V_{CM} and V_{DM} as

$$V_{AN} = V_{CM} + \frac{V_{DM}}{2} \quad (3)$$

$$V_{BN} = V_{CM} - \frac{V_{DM}}{2} \quad (4)$$

$$V_{ECM} = V_{CM} + \frac{V_{DM}}{2}\frac{L2 - L1}{L1 + L2} \quad (5)$$

Since identical filter inductors (L1 =L2) are use dint is Paper, the VECM is equal to VCM

$$V_{ECM} = V_{CM} = \frac{V_{AN} + V_{BN}}{2} \quad (6)$$

From the model, it can be concluded that the leakage current is very much dependent of the CMV. Thus, converter structure and the modulation technique must be designed to generate constant CMV in order to eliminate the leakage current. It is worth highlighting that the model in Fig1(c) has been commonly used for describing the common-mode behavior of the conventional full-bridge (H4) topology. However, due to the generality of the model, it is obvious that the model is valid for other topologies discussed here, apart from H4. As a matter of fact, the same model has been used to analyze the common-mode behavior of various transformers less converter topologies. However, since different topology has different VAN and VBN, the expressions for VCM and VDM will differ from one another,

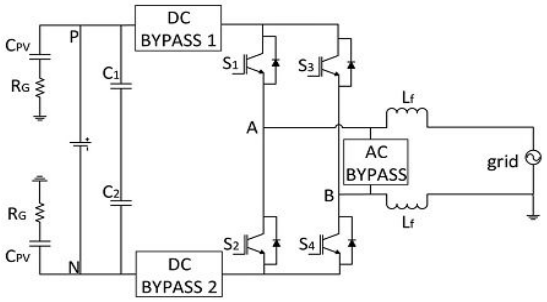

Fig.2. Universal transformer less topologies. Common-mode behavior. Hence, to evaluate the common mode.

International Journal for Innovative Engineering and Management Research
A Peer Revieved Open Access International Journal
www.ijiemr.org

Behavior of a particular topology, VAN and VBN under different switching condition need to be evaluated, as will be shown later.

A. Galvanic Isolation

In transformed less PV inverters, the galvanic connection between the PV and the grid allows leakage current to flow. Hence, in topologies such as H5 and HERIC, galvanic isolation is provided to reduce the leakage current. The galvanic isolation can basically be categorized into dc-decoupling and ac-decoupling methods. For dc-decoupling method, dc-bypass switches are added on the dc side of the inverter to disconnect the PV arrays from the grid during the freewheeling period.

However, the dc-bypass branch, which consists of switches or diodes, is included in the conduction path as shown in Fig.3. For H6, output current flows through two switches and the two dc-bypass branches during the conduction period. Hence, the conduction losses increase due to the increased number of semiconductors in the conduction path. On the other hand, bypass branch can also be provided on the ac side of the inverter (i.e., ac-decoupling method) such as seen in HERIC.

This ac-bypass branch functions as a freewheeling path which is completely isolated from the conduction path, as shown in Fig.2. As a result, the output current flows through only two switches during the conduction period. Therefore, topologies employing ac-decoupling techniques are found to be higher in efficiency as compared to dc-decoupling topologies. One setback of galvanic isolation is that there is no way of controlling the CMV by PWM during the freewheeling period. Fig.3. shows operation modes of galvanic isolation which

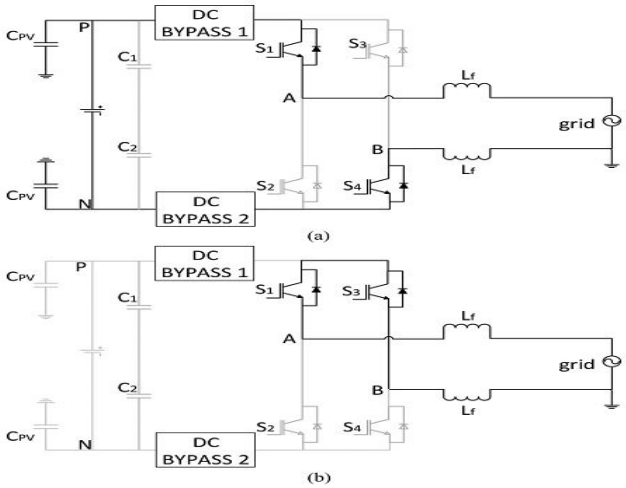

Fig.3. Operation modes of dc-decoupling topology. (a) Conduction mode and (b) freewheeling mode.

Employs dc-decoupling method. As shown in Fig.3 (a), during the conduction period, S1 and S4 conduct to generate the desired output voltage. At the same time, VA is directly connected to VDC and VB is connected to the negative terminal (N) of the dc-link. Hence, the CMV becomes.

$$V_{CM} = \frac{V_{AN} + V_{BN}}{2} = \frac{1}{2}(V_{DC} + 0) = \frac{V_{DC}}{2} \quad (7)$$

Nevertheless, during the freewheeling period, the dc-bypass switches disconnect the dc-link from the grid. Therefore, point A and point Bare isolated from the dc-link, and VA and VB are floating with respect to the dc-link as shown in Fig.3 (b). The CMV during this period of time is not determined by the switching state, but instead, is oscillating with amplitude depending on the parasitic parameters and the switches' junction capacitances of the corresponding topology. As a result, leakage current can still flow during freewheeling period. The same is the case for converters using ac-decoupling method.

International Journal for Innovative Engineering and Management Research
A Peer Revieved Open Access International Journal
www.ijiemr.org

B.CMV Clamping

As mentioned earlier, CMV is one of the main causes for leakage current. H5 and HERIC focus only on providing galvanic isolation while neglecting the effect of the CMV. Unlike conventional topologies, the CMV in these topologies cannot be manipulated via PWM, due to the use of galvanic isolation as explained previously. In order to generate constant CMV clamping branch is introduced in oH5.

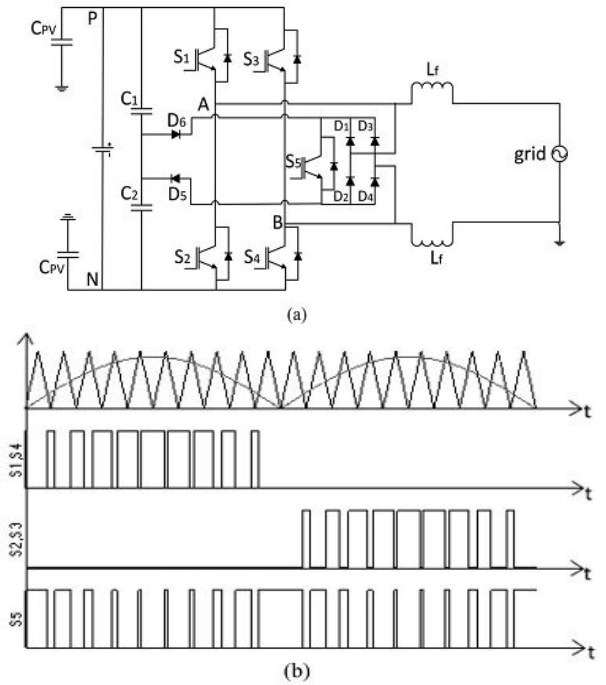

Fig.4. Proposed HBZVR-D topology. (a) Converter structure. (b) Switching Waveforms.

Generally, the clamping branch consists of diode or switches and a capacitor divider which ensures the freewheeling path is clamped to the half of the input voltage. With the combined effect of galvanic isolation and CMV clamping, leakage current is completely laminated. Nevertheless, both H6 and oH5 uses dc-decoupling method, which suffers from lower efficiency. HBZVR also employs CMV clamping technique but it is found that the clamping branch does not function optimally. It is shown in both the simulation and experimental results that the CMV and the leakage current in HBZVR are as high as those in the topologies which use only galvanic isolation.

III. OPERATION PRINCIPLES OF PROPOSED TOPOLOGY

A. Structure of Proposed HBZVR-D

Based on the analysis above, a simple modified HBZVR-D is proposed to combine the benefits of the low-loss ac-decoupling method and the complete leakage current elimination of the CMV clamping method. HBZVR-D is modified by adding a fast-recovery diode, D6, to the existing HBZVR as shown in Fig 4 (a). The voltage divider is made up of C1and C2.S1−S4 are the for full-bridge inverter. The anti-parallel diodes, D1−D4, as well as S5 provide a freewheeling path for the current to flow during the freewheeling period. DiodesD5 and D6form the clamping branches of the freewheeling path.

B. Operation Modes and Analysis

In this section, the operation modes and the CMV of the proposed topology is discussed. Fig.4 (b) illustrates the switching (c) Mode 3—conduction mode and (d) Mode 4—freewheeling mode during negative half cycle Patterns of the proposed HBZVR-D.

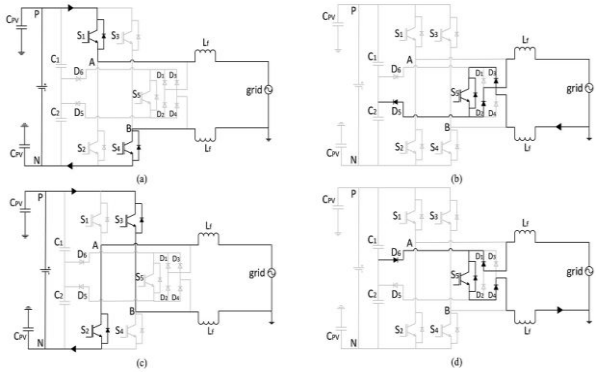

Fig.5. Operation modes of proposed HBZVR-D topology. (a) Mode 1—conduction mode and (b) Mode 2—freewheeling mode during positive half cycle.

International Journal for Innovative Engineering and Management Research
A Peer Revieved Open Access International Journal
www.ijiemr.org

SwitchesS1−S4 commutate at switching frequency to generate unipolar output voltage. S5 commutates complementarily to S1−S4 to create freewheeling path. All the four operation modes are shown in Fig.6. To generate unipolar output voltage. In mode 1,S1 andS4 are ON while S2,S3 and S5 are OFF. Current increases and flows throughS1andS4.VAB=+VDC. The CMV becomes

$$V_{CM} = \frac{V_{AN} + V_{BN}}{2} = \frac{1}{2}(V_{DC} + 0) = \frac{V_{DC}}{2}. \quad (8)$$

In mode 2, S1−S4are OFF.S5is ON to create a freewheeling Path. Current decreases and freewheels through diodesD3, and the grid. The voltage VAN decreases and VBN increases until their values reach the common point, VDC/2, such that VAB=0. The CMV is

$$V_{CM} = \frac{V_{AN} + V_{BN}}{2} = \frac{1}{2}\left(\frac{V_{DC}}{2} + \frac{V_{DC}}{2}\right) = \frac{V_{DC}}{2}. \quad (9)$$

In mode 3, S2 andS3 are ON, whileS1, S4 andS5 are OFF. Current increases and flows throughS2andS3.VAB=−VDC. The CMV becomes

$$V_{CM} = \frac{V_{AN} + V_{BN}}{2} = \frac{1}{2}(0 + V_{DC}) = \frac{V_{DC}}{2}. \quad (10)$$

In mode 4, S1−S4are OFF.S5is ON to create freewheeling path. Current decreases and freewheels through diodesD1, D4, and the grid. The voltage VAN decreases and VBN increases until their values reach the common point, VDC/2, and VAB=0. The CMV is as derived in (10). Obviously, modulation techniques are designed to generate Constant CMV in all four operation modes. All the research Works are designed based on the principles above. Practically, VAN and VBN do not reach common point during the freewheeling period (mode 2 and mode 4). It is shown in simulation and experimental results later that the CMV is not constant without clamping branch. During the freewheeling period, both VAN and VBN are not clamped to VDC/2 and is oscillating with amplitude depending on the parasitic parameters and junctions' capacitance of those topologies. The improved clamping Branch of HBZVR-D ensures the complete clamping of CMV to VDC/2 during the freewheeling period. It is well noted that the Output current flows through only two switches in every conduction period (mode 1 and mode 3) as shown in Fig.6.(a) and (c). This explains why HBZVR-D has relatively higher efficiency than those of dc-decoupling topologies.

C. Operation Principles of Improved Clamping Branch

During the freewheeling period, S5 is turned ON, connecting Point A and B. Freewheeling path voltage VFP can be defined as VFP=VAN≈VBN, since the voltage drops across diodes and S5 are small compared to VDC. There are two possible modes of operation (mode 2 and mode 4 as shown in Fig.6) depending on whether D5 or D6 is forward biased. When VFP is greater Than VDC/2, D5 is forward biased and D6 is reversed biased. Current flows from the freewheeling path to the midpoint of the dc-link via the clamping diode D5, as shown in Fig.6 (b), which completely clamps the VFP to VDC/2. On the other hands, when the VFP is less than VDC/2, D6 is forward biased and D5is reversed biased. As shown in Fig.6 (d), current flows from the midpoint of the dc-link to the freewheeling path via the added clamping diodeD6, to increase the VFP to VDC/2. It should be noted that during the dead time between the conduction period and freewheeling period, the freewheeling path is not well-clamped and the CMV can be oscillating with the grid voltage. Nevertheless, with proper selection of dead time, this effect can be

International Journal for Innovative Engineering and Management Research
A Peer Revieved Open Access International Journal
www.ijiemr.org

minimized. In HBZVR, the clamping branch consists of D5 only. Thus, the clamping of the freewheeling path is limited only for the period when VFP is more than VDC/2. When VFP is less than VDC/2, the clamping branch does not function because D5 is reversing biased. During such condition, the CMV in HBZVR will oscillate, causing the flow of leakage current. This setback is rectified by adding a fast-recovery diodeD6 in the Proposed HBZVR-D topology. With both D5 and D6, the improved clamping branch guarantees the complete clamping of the CMV to VDC/2 throughout the freewheeling period. As a result, leakage current, which is very much dependent on CMV, is completely eliminated.

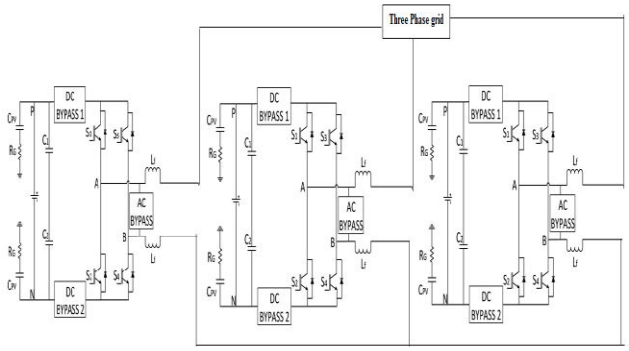

Fig.7.Three-phase transformer less PV inverters.

IV.MATLAB/SIMULATION RESULTS

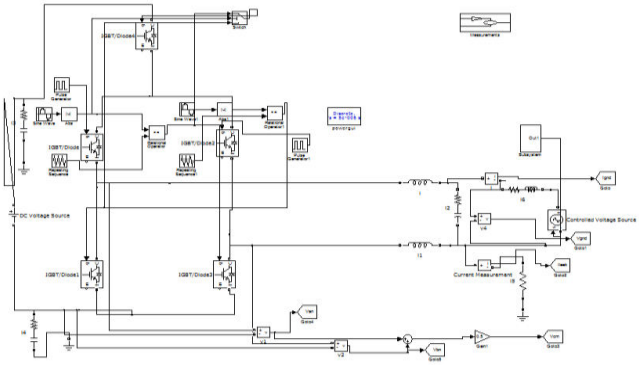

Fig.8.Matlab/Simulation model of H5 Topology.

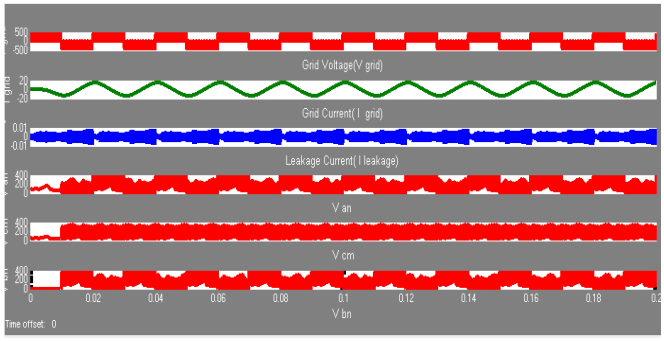

Fig.9.Simulation results OF grid voltage and Current, leakage Current, Van, Vcm, Vbn of H5 Topology.

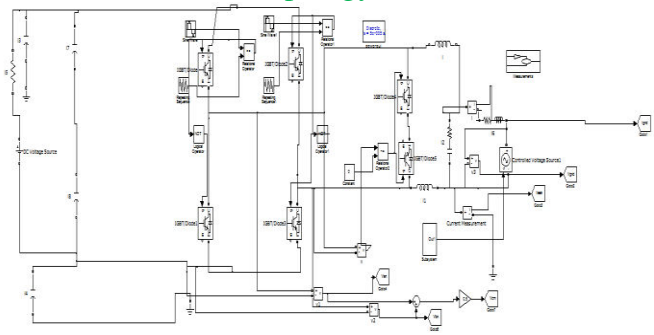

Fig.10.Matlab/Simulation model of HERIC topology.

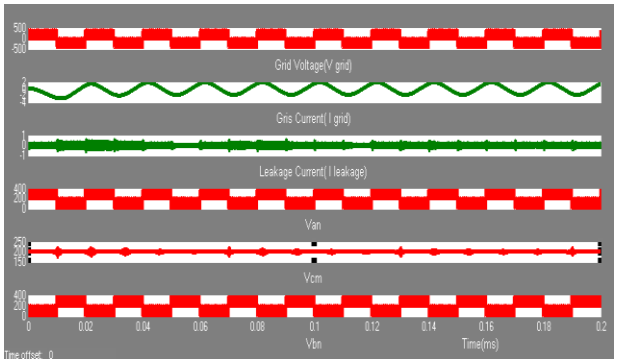

Fig.11.Simulation results of grid voltage and Current, leakage Current, Van, Vcm, Vbn of HERIC Converter.

International Journal for Innovative Engineering and Management Research
A Peer Revieved Open Access International Journal
www.ijiemr.org

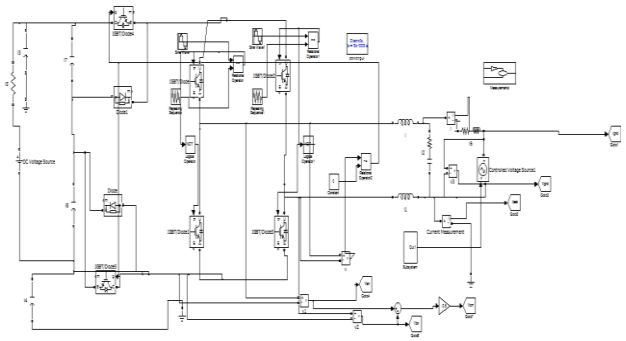

Fig.12.Matlab/simulation model of OH5 Topology.

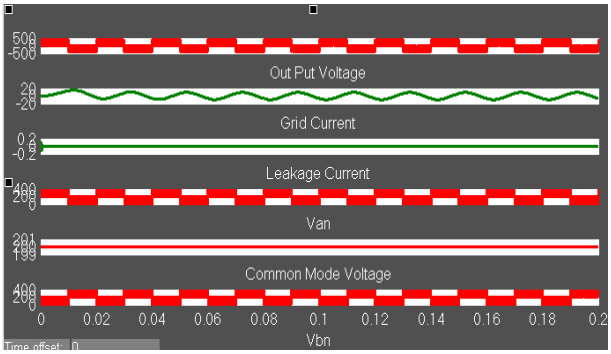

Fig.13.Simulation results for output Voltage, Grid Current, leakage Current, Van, Common mode Voltage and Vbn OH5 Topology.

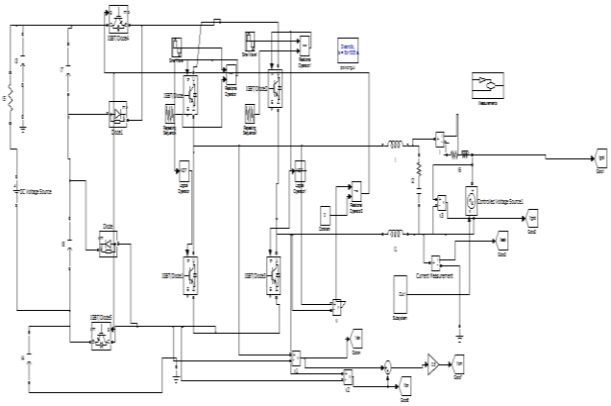

Fig.14.Matlab/simulation model of H6 Topology.

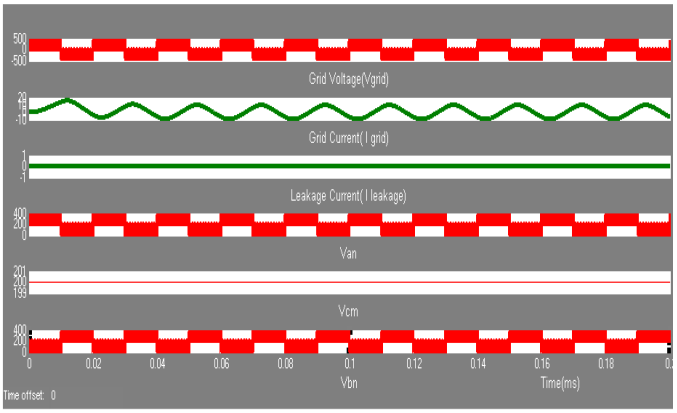

Fig.15.Simulation results of grid voltage and Current, leakage Current, Van, Vcm, Vbn of H6 Converter.

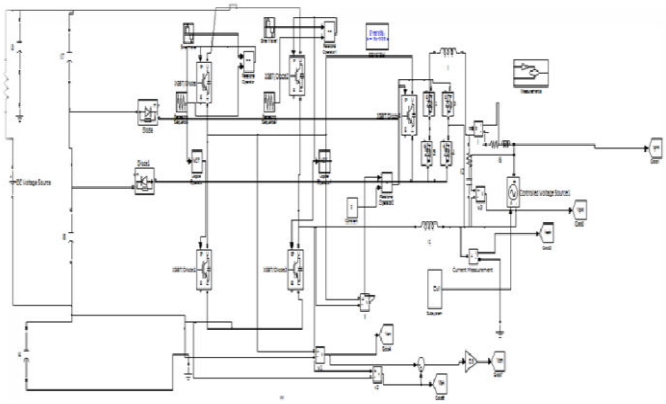

Fig.16.Simulation Model of HBZVR Topology.

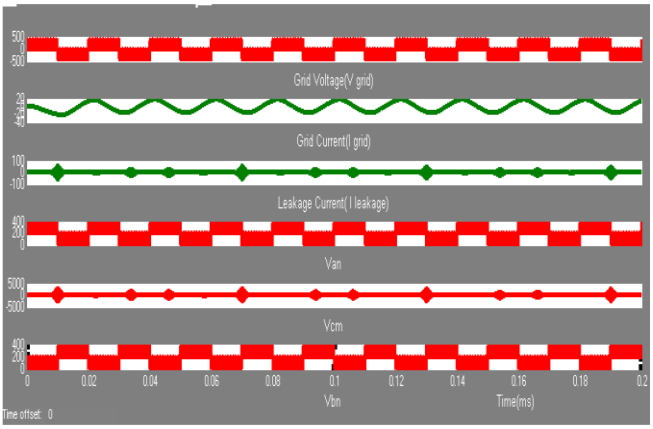

Fig.17.Simulation results of grid voltage and Current, leakage Current, Van, Vcm, Vbn of HBZVR Converter.

International Journal for Innovative Engineering and Management Research
A Peer Revieved Open Access International Journal
www.ijiemr.org

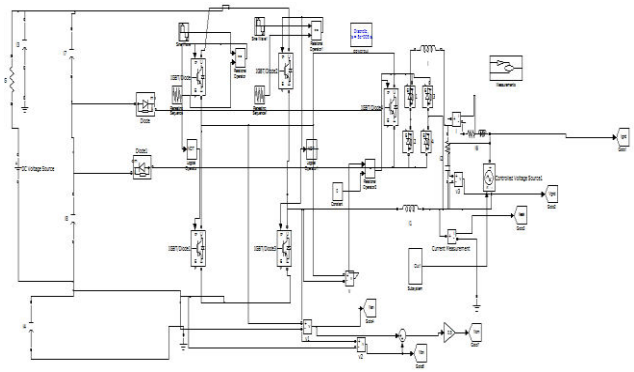

Fig.18.Matlab/simulation model of HBZVR-D Topology.

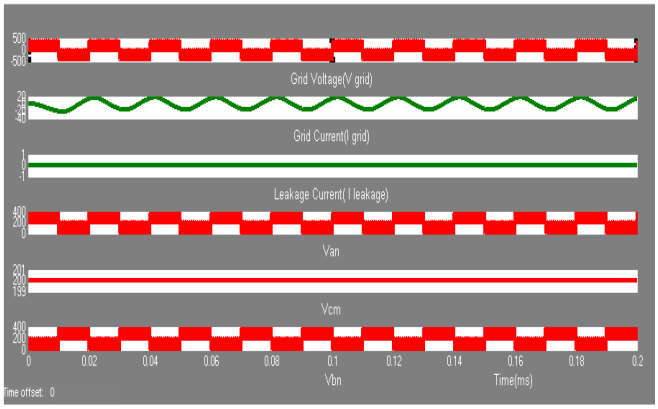

Fig.19.Simulation results of grid voltage and Current, leakage Current, Van, Vcm, Vbn of HBZVR-D Converter.

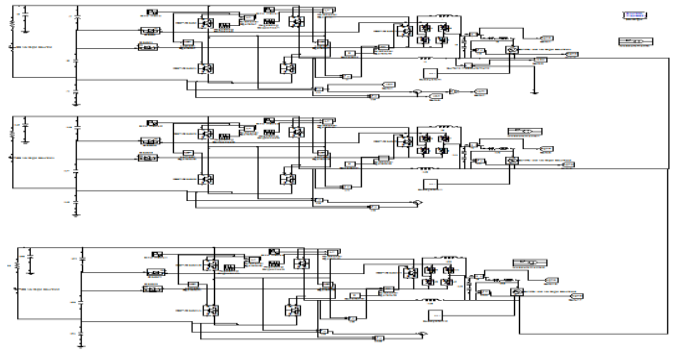

Fig.20.Simulation model of Three-level three-phase PV inverter topology.

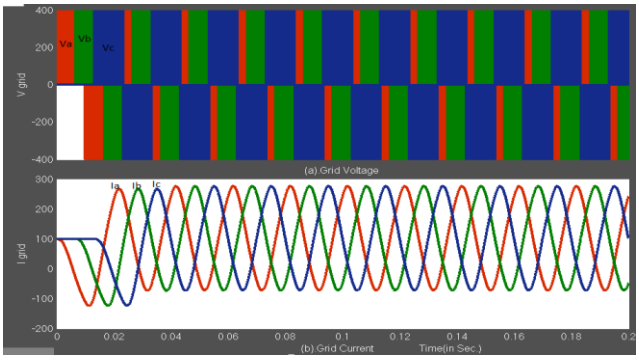

Fig.21.Grid voltage and grid current in three level three-phase full-bridge transformer less PV Inverter.

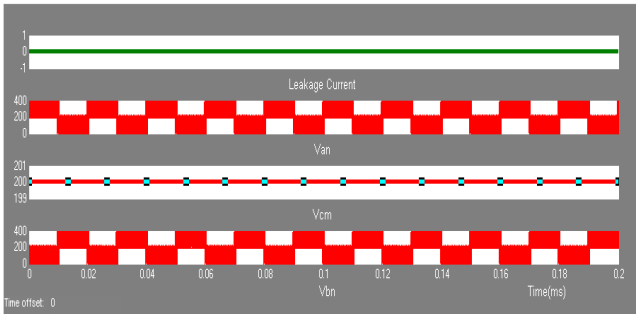

Fig.22.CMV and Leakage Current in three-level three phase transformer less PV Inverters.

V.CONCLUSION

The performance of paper implemented in the three phase grid connected. A high reliability and efficiency inverter for transformer less PV grid-connected power generation systems is presented in this paper. Ultra high efficiency can be achieved over a wide output power range by reliably employing super junction MOSFETs for all switches since their body diodes are never activated and no shoot-through issue leads to greatly enhanced reliability. Low ac output current distortion is achieved because dead time is not needed at PWM switching commutation instants and grid-cycle zero-crossing instants. The higher operating frequencies with high efficiency enables reduced cooling requirements and results in system cost savings by shrinking passive components. The proposed converter

three phase grid connected. The patented works, such as H5 and HERIC, provide galvanic isolation for safety purposes. Nevertheless, their CMVs are not clamped and leakage currents are not completely eliminated .Other topologies, such as oH5 and H6, eliminate the leakage current with the use of both galvanic isolation and CMV clamping, at the expense of reduced system efficiency. By using ac-decoupling method instead of dc-decoupling method for galvanic isolation, HBZVR and HERIC manage to achieve higher efficiency than the rest but perform poorly in terms of common mode behavior. With the understanding on the merits and demerits of the different approaches, a modified HBZVR topology is obtained by addition of a fast-recovery diode. The proposed topology (known as HBZVR-D) combines the advantages of the low loss ac-decoupling method and the complete leakage current elimination of the CMV clamping method. The performance of the transformer less topologies, including the proposed HBZVR-D, is compared in terms of CMV, leakage current, losses, THD, and efficiency. It is experimentally proven that HBZVR-D topology gives the best overall performance and is suitable for transformer less PV applications for a 230-V (rms) grid system.

REFERENCES

[1] F. T. K. Sudan, N. A. Rahim, and H. W. Ping, "Modeling, analysis and control of various types of transformer less grid connected PV inverters ,in Proc. IEEE Clean Energy Technol., Jun. 2011, pp. 51–56.

[2] N. A. Rahim, K. Chan ago, and J. Selvaraj, "Single-phase seven-level grid connected inverter for photovoltaic system, "IEEE Trans. Ind. Electron vol. 58, no. 6, pp. 2435–2443, Jun. 2011.

[3] G. Petrone, G. Spagnuolo, R. Teodorescu, M. Veerachary, and M. Vitelli, "Reliablility issues in photovoltaic power processing systems," IEEE Trans. Ind. Electron., vol. 55, no. 7, pp. 2569–2580, Jul. 2008.

[4] M. Calais, J. Myrzik, T. Spooner, and V. G. Agelidis, "Inverters for single-phase grid connected photovoltaic system – an overview," in Proc. IEEE Power Electron. Spec. Conf., 2002, pp. 1995–2000.

[5] J. M. Shen, H. L. Jou, and J. C. Wu, "Novel transformer less grid connected power converter with negative grounding for photovoltaic generation system," IEEE Trans. Power Electron., vol. 27, no. 4, pp. 1181– 1829, Apr. 2012.

[6] S. V. Araujo, P. Zacharias, and R. Mallwithz, "Highly efficient single phase transformer less inverters for grid-connected photovoltaic systems," IEEE Trans. Ind. Electron., vol. 57, no. 9, pp. 3118–3128, Sep. 2010.

[7] O. Lopez, F. D. Freijedo, A. G. Yepes, P. Fernandez-Comesaa, J. Malvar, R. Teodorescu, and J. Doval-Gandoy, "Eliminating ground current in a transformer less photovoltaic application, "IEEE Trans. Energy Convers., vol. 25, no. 1, pp. 140–147, Mar. 2010.

[8] T. Kerekes, R. Teodorescu, M. Liserre, C. Klumpner , and M. Sumner, "Evaluation of three-phase transformer less photovoltaic inverter topologies, "IEEE Trans. Power Electron., vol. 24, no. 9, pp. 2202–2211, Sep. 2009.

[9] B. N. Alajmi, K. H. Ahmed, G. P. Adam, and B. W. Williams, "Single phase single-stage transformer less grid-connected PV system," IEEE Trans. Power Electron., vol. 28, no. 6, pp. 2664–2676, Jun. 2013.

[10] Y. Gu, W. Li, Y. Zhao, B. Yang, C. Li, and X. He, "Transformer less inverter with virtual DC bus concept for cost-effective grid-connected

PV power systems, "IEEE Trans. Power Electron., vol. 28, no. 2, pp. 793–805, Feb. 2013.

[11] D. Meneses, F. Blaabjerg, O. Garc´ıa, and J. A. Cobos, "Review and comparison of step-up transformer less topologies for photovoltaic ac-module application, "IEEE Trans. Power Electron., vol. 28, no. 6, pp. 2649–2663, Jun. 2013.

[12] L. Zhang, K. Sun, L. Feng, H. Wu, and Y. Xing, "A family of neutral point clamped full-bridge topologies for transformer less photovoltaic grid-tied inverters, "IEEE Trans. Power Electron., vol. 28, no. 2, pp. 730–739, Feb. 2013.

[13] E. Koutroulis and F. Blaabjerg, "Design optimization grid-connected PV inverters including reliability," IEEE Trans. Power Electron., vol. 28, no. 1, pp. 325–335, Jan. 2013.

[14] Automatic Disconnection Device between a Generator and the Public Low-Voltage Grid, DIN Electro technical Standard DIN VDE 0126–1–1, 2005.

AUTHORS

Mr.VANTALA SIVA LINGAM received the Bachelor of Engineering Degree in Electrical & Electronics Engineering from Gnyana Saraswathi College of Engineering and Technology, Nizamabad from JNTU Hyderabad in 2011. Currently he is pursuing Master of Technology in Chaitanya Institute of Science & Technology,Kakinada,A.P. His areas of interests are in Electrical and Electronic Measurements and Instrumentation, Power Systems, Power Electronics and Electrical Machinery Modeling and Analysis, Power Quality.

Mr. D.PRAKASA RAO received the Bachelor of Engineering degree in Electrical & Electronics Engineering from CIST, Madhavapatnam from JNTU Kakinada in 2010. He received master of technology from Sai Aditya Institute of Science&Technology, Surumpalem,A.P., in 2014, He is currently working as assistant professor in Chaitanya Institute of Science & Technology, Kakinada, A.P. His areas of interests are in Power Systems, Power Electronics and Machines,Electrical Circuits.

Mr. M.PAPAYYA NAIDU,
M.Tech.,Professor,Head of The Department,EEE, CHAITANYA INSTITUTE OF SCIENCE & TECHNOLOGY, KAKINADA,ANDHRA PRADESH.INDIA.